Chemical Engineering Journal 473 (2023) 145452

Contents lists available at ScienceDirect

Chemical Engineering Journal

journal homepage: www.elsevier.com/locate/cej

An interfacial solar evaporation enabled autonomous double-layered vertical floating solar sea farm

Pan Wu [a,b], Xuan Wu [b], Huimin Yu [b], Jingyuan Zhao [b], Yida Wang [b], Kewu Pi [a], Gary Owens [b,*], Haolan Xu [b,*]

[a] Innovation Demonstration Base of Ecological Environment Geotechnical and Ecological Restoration of Rivers and Lakes, School of Civil and Environmental Engineering, Hubei University of Technology, Wuhan, Hubei 430068, China

[b] Future Industries Institute, University of South Australia, Mawson Lakes Campus, SA 5095, Australia

ARTICLE INFO

Keywords:
Interfacial solar evaporation
Desalination
Vertical farming
Solar sea farm
Sustainable agriculture

ABSTRACT

Water, energy, and food security are the three most critical elements for achieving the 2030 United Nations' Sustainable Development Goals. While much effort has been focused on the development of interfacial solar evaporation technology for seawater desalination, limited effort has been directed towards potential sustainable agricultural applications. This work addresses this gap by developing a self-sustaining and solar-driven offshore double-layered sea farm system to address growing global shortages in clean water, agricultural land resources and food supply. During a long-term field test, this unique design was used to successfully germinate and grow, with a survival rate of 80%, three common vegetable crops (broccoli, lettuce, and Pak Choi) on seawater surfaces without maintenance nor additional clean water irrigation. Thus, this design could potentially make a significant contribution to sustainable agriculture production in the seawater-energy-food nexus.

1. Introduction

Clean water and food are the two most strategically important resources essential for human survival and growth of civilization. It is reported that by 2050, the population affected by freshwater shortages will increase from 933 million in 2016 to as much as 2.37 billion, where simultaneously global supply of water for agriculture irrigation is expected to decline by ~19% [1]. Thus to sustainably feed the increasing population (estimated to reach 10 billion by 2050), food productivity must be significantly improved while simultaneously reducing the impact of agriculture on fragile ecosystems is required to ensure that agriculture promotes inclusive economic development [2–5]. Recent research indicates that autonomous environmental water-harvesting technologies can potentially satisfy water demands for both agricultural and human beings [6–11]. For example, Tan's team demonstrated ambient moisture harvest for autonomous urban agriculture [1,12,13]. Wang's group also showed the utilization of waste heat from photovoltaic panels to produce fresh water from the atmosphere for crop irrigation [3,14]. Therefore, harnessing energy from the surrounding environment as an alternative water production approach can be a promising strategy to address water shortages and realize agricultural sustainability. In addition to the direct reduction in available clean water for agriculture, the declining arable land suitable for agriculture has further exacerbated food security. Crop production currently occurs on 11% of the world's land, which only accounts for 3% of the planet's surface area [15]. It is exciting that the ocean (70% of the earth's surface area) now provides a new frontier and opportunity for a new kind of agricultural development. If it can be utilized effectively and rationally, marine agriculture could play a pivotal role in combating climate change and simultaneously addressing the food and clean water shortages [16,17].

Although marine agriculture has already been developed to some extent, it currently faces several issues and has some major limitations. Firstly, marine agriculture is mainly suitable only for specialized aquatic and some salt-tolerant hydroponic plants, which by themselves would not be able to meet growing global food demands. Secondly, due to limited freshwater resources in marine areas, additional freshwater production facilities are normally required to be collated to support plant irrigation, which is extremely costly and requires frequent supervision and ongoing maintenance, limiting its extensive applications [13]. In addition, clean water and crop production are typically physically separated into individual operational units that occupy a large

* Corresponding authors.
E-mail addresses: gary.owens@unisa.edu.au (G. Owens), haolan.xu@unisa.edu.au (H. Xu).

https://doi.org/10.1016/j.cej.2023.145452
Received 14 June 2023; Received in revised form 3 August 2023; Accepted 13 August 2023
Available online 15 August 2023

amount of surface area, thus increasing overall maintenance and operation costs. Therefore, there is an urgent need to develop a completely new strategy for the practical application of marine agriculture that is applicable to a wide variety of commercial crop types, efficient in clean water supply, easy to operate, and economically viable. Interfacial solar evaporation (ISE) has recently received extensive research interest owing to the abundance of both solar energy and seawater, as well as its minimal environmental impact [18–33]. It has been recognized as a promising technology for seawater desalination, atmospheric moisture harvesting and release, solar panel cooling, and soil remediation [34–52]. The main advantage relative to previously developed technologies is that ISE-based desalination technology creates a self-sustainable source of clean water that has the potential to not only support millions of people's drinking water needs but also increase agricultural needs [13,53,54]. Recently, our group applied solar light and seawater for saline soil remediation and irrigation, successfully demonstrating that a self-sustainability of a combined ISE desalination-agriculture system was possible [34]. Hence, ISE technologies could also be a potential new strategy for addressing marine agricultural freshwater shortages.

In this work, a multifunctional double-layered vertical solar sea farm (DVSSF) was developed which achieved self-priming irrigation by ISE of seawater (bottom layer) and agricultural cultivation (top layer) through longitudinal stratification. This solution substantially improves the sea surface area utilization to ensure sustainable clean water production for agricultural use (Fig. 1a). The bottom layer of the DVSSF is the clean water production chamber (Fig. 1b), which simply uses ISE technology to effectively evaporate seawater under solar irradiation to generate clean water. Water transportation belts that connect the two chambers enable continuous transportation of condensed clean water from the bottom evaporation chamber to the upper soil-containing chamber. Outdoor experiments showed that three different common vegetables (broccoli, lettuce and Pak Choi) could all grow well on the seawater surfaces with a germination rate > 80%. Thus, with minimal geological constraints and maintenance, this DVSSF can effectively alleviate the dilemma of insufficient supply of agricultural products caused by current ongoing reductions in the availability of both per capita clean water supply and arable land, which will provide a promising means to facilitate modern marine agriculture.

2. Materials and methods

2.1. Material and chemicals

Reduced graphene oxide (rGO) was provided by Huasheng Graphite Co., Ltd., China. Towel (TW) was purchased from a local supermarket. Tannic acid (TA) and ferrous chloride were purchased from Sigma-Aldrich. Broccoli seeds (*Italian Sprouting*), lettuce seeds (*Country Value Little Gem Lactuca sativa*) and Pak Choi (*Brassica rapa* Var. *chinensis*) seeds were obtained from a local market. Agricultural soil was supplied by a local farm. Soil properties were introduced in our previous work [55] and provided here in Table S1.

2.2. Fabrication of rGO-TA-TW

Photothermal rGO-TA-TW was fabricated using rGO, TA and TW. Due to the strong and quick coordination between the phenolic hydroxyl groups of TA and Fe^{3+}, a black complex of TA-Fe^{3+} can readily be formed when mixing the TA and Fe^{3+} [52,56], where to further enhance light absorption, rGO was also added. Initially, 0.5 g TA powder was mixed with an rGO suspension (0, 0.1, 0.3, 0.5, 1.0 mg mL^{-1}, 100 mL) and stirred continuously at 500 rpm for 12 h. Thereafter, the homogeneous suspension was dropped onto the surface of tailored TW (25 cm width × 30 cm length). The modified rGO-TA-TW was then freeze dried for 48 h at −60 °C before being immersed in 5% $FeCl_3$ (500 mL) for another 12 h to facilitate crosslinking. After washing with Milli-Q water and freeze drying again at −60 °C for another 48 h, the final photothermal rGO-TA-TW was obtained.

2.3. Materials characterization

The hydrophilicity of TW and rGO-TA-TW was characterized using a contact angle system (Data physics OCA 20). The microstructure of TW and rGO-TA-TW was imaged using scanning electron microscopy (SEM) on a Zeiss Merlin scanning electron microscope. Concentrations of cations in seawater and condensed water were determined using inductively coupled plasma optical emission spectrometry (ICP-OES, Agilent 7500).

2.4. Solar-driven seawater evaporation tests

With the exception of the long-term tests, all solar seawater evaporation tests were conducted under controlled laboratory conditions (i.e., temperature ~ 25 °C and relative humidity ~ 34%). A Newport Oriel solar simulator (class ABA, 450 W, 69920) was used to provide 1.0 sun illumination during indoor tests. A THORLABS PM400 optical power meter was used to measure and calibrate the intensity of the simulated solar light. During solar evaporation, evaporated water was recorded using an electronic balance. An infrared camera (FLIRE64501) was used to measure the temperature of evaporation surfaces.

2.5. Long-term germination test

Long-term solar evaporation-based cropping was investigated within

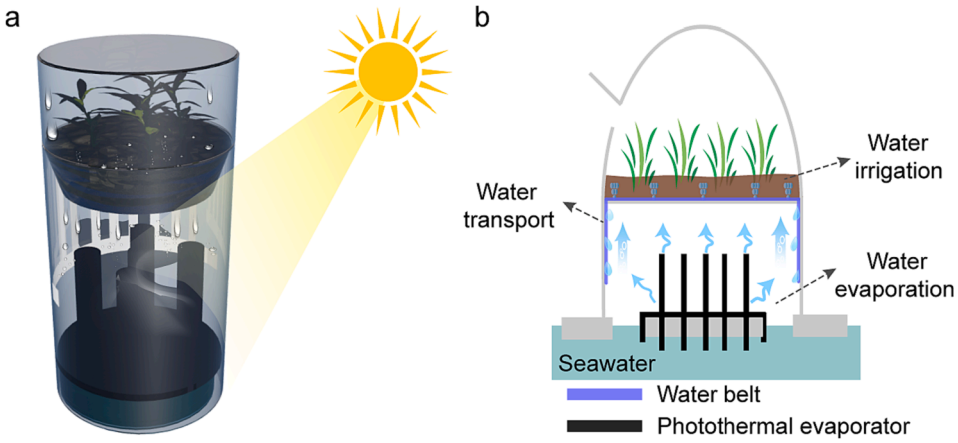

Fig. 1. (**a**) Schematic illustration of the autonomous DVSSF. (**b**) Cross-sectional view of autonomous DVSSF.

a DVSSF. The DVSSF system integrated three subsystems, 1) a solar evaporator system (bottom layer), 2) a water condensation and transfer system (water belts), and 3) a plant cultivation system (top layer). The solar evaporation system was composed of photothermal evaporators and polystyrene (PS) foam with holes as the evaporator support. During practical operation, the PS foam floated on the water surface and a small part of the photothermal evaporator was immersed in the bulk water to enable water transport to the evaporation surfaces (Fig. 1a, b). A solar simulator (Newport Oriel Xenon Lamp, 66485-300XF-R1) with adjustable incident light angle provided simulated sunlight. For water condensation and transportation, hydrophilic belts (bamboo paper) were vertically arranged on the inner side surface of the cylindrical container (10 cm radius, 25 cm high) and across the bottom and top chambers. For the upper cultivation chamber, a transparent cover was used to cover the soil (similar to a greenhouse). The water transportation belts adsorb the condensed vapor in the bottom solar evaporation chamber and transfer the clean water to the upper soil chamber for plant irrigation.

2.6. Outdoor optimization experiments

Outdoor experiments with four identical experimental setups were conducted between 1st and 14th March 2022 at the Mawson Lakes Campus, University of South Australia, Adelaide, Australia. An integrated temperature and humidity meter was used to monitor the temperature and humidity outside and inside the planting chamber. During pot cultivation, the soil water evaporation was controlled by adjusting the open rate of the transparent cover. In addition, ambient daily solar flux and other environmental conditions, such as environmental temperature and humidity, were collected from a local Meteorological monitoring stations close to the experimental site [34].

2.7. Outdoor scale-up tests

Outdoor scale-up experiments were conducted over 20 days in a large pool (1 m^2) filled with 300 L of artificial seawater. Six DVSSFs containing seeds of broccoli, lettuce, and Pak Choi were prepared and spaced 10 cm apart. A PS foam board was used as a support to float the DVSSFs on the water surfaces.

3. Results and discussion

3.1. Materials design and solar driven seawater evaporation

Creating a surface with both high light absorption and light-to-heat conversion efficiency is crucial for achieving high clean water production via ISE. Here due to strong and rapid coordination between the phenolic hydroxyl groups of TA and Fe^{3+}, TA crosslinked with Fe^{3+} can firmly adhere on the surfaces of substrates with different shapes and surface chemistries [52,56]. Additionally, inclusion of rGO into the crosslinked complex can further increase the light absorption capability which benefits ISE. Coating of the cotton TW with rGO-TA changed the surfaces of the TW fibers (Fig. 2a-d and Fig. S1). The initial smooth surfaces of the TW fibers (Fig. 2a, b) became rougher and the gaps between the fibers were filled with both rGO and TA after the coating process (Fig. 2c, d). The light absorption of rGO-TA-TW increased with an increase in rGO concentration. For example, the light absorption of pristine TW was only 44.6%, which increased significantly to 85.5% when the rGO concentration was increased to 0.5 mg L^{-1}. The light absorption of the wet rGO-TA-TW (wet sample aligned better with the

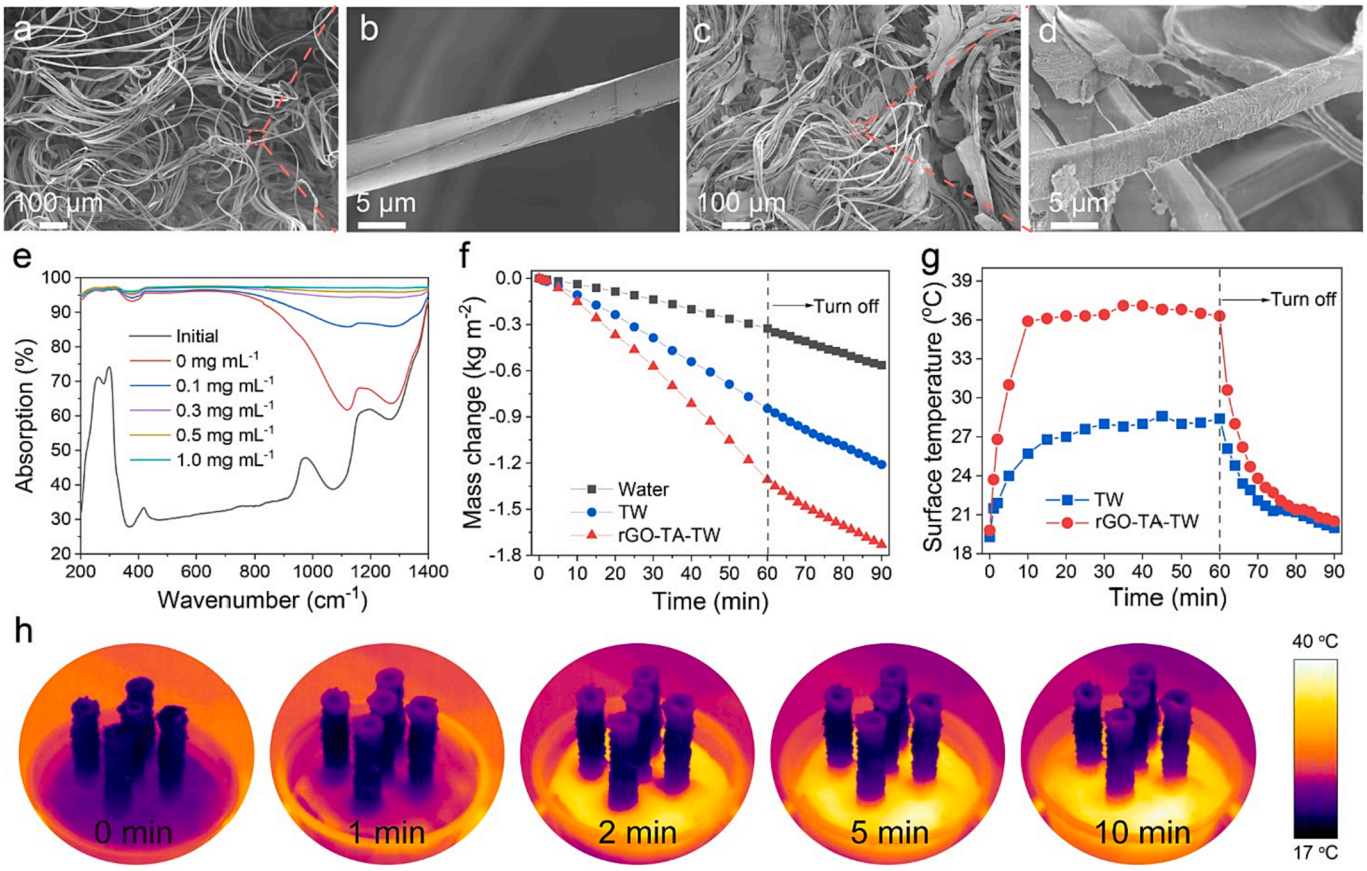

Fig. 2. Materials characterization and solar seawater evaporation test. (**a, b**) SEM images of the initial TW. (**c, d**) SEM images of rGO-TA-TW. (**e**) Light absorption of rGO-TA-TW with different rGO concentrations. (**f**) Water mass change under one sunlight illumination for 60 min and after light-off for 30 min. (**g**) Surface temperature under one sun illumination for 60 min and after light-off for 30 min. (**h**) IR images of the evaporators during solar evaporation under one sun illumination.

practical conditions during solar evaporation) further increased to 96.7% (Fig. 2e). In addition, rGO-TA-TW was highly hydrophilic. A water droplet could be quickly absorbed within 0.6 s. While for pristine TW, it took about 4 s for water adsorption (Fig. S2). Moreover, rGO-TA-TW also showed excellent stability, being able to withstand 10 min of continuous sonication with no black materials being flaked off (Fig. S3). The introduction of photothermal materials significantly improved water evaporation performance. The solar evaporation rate of seawater using the rGO-TA-TW under 1.0 sun was 1.29 kg m^{-2} h^{-1} (Fig. 2f), which was about 4 times higher than that without rGO-TA-TW (i.e., only seawater). The pillar-like structure of the evaporator could increase overall evaporation surface area and light absorption. During solar evaporation, the surface temperature of the wet rGO-TA-TW could quickly reach a steady temperature of 36 °C within 10 min to accomplish rapid solar heat localization and efficient ISE (Fig. 2g, h). When solar radiation ceased, rGO-TA-TW swiftly cooled to room temperature within 30 min. As the temperature gradually decreased, the evaporation rate also decreased. In comparison, water and pristine TW showed a poor photothermal effect with equilibrium surface temperatures < 24 °C, due to their relatively low light absorption (Fig. S4-5).

3.2. Clean water collection and soil irrigation

In this system, generated vapor can be condensed and collected as clean water for subsequent plant irrigation. An enclosed solar evaporation system was used to estimate vapor condensation rate/clean water collection rate (Note: solar evaporation rate doesn't mean clean water collection rate) (Fig. S6). During 8 h of continuous solar evaporation, the pristine TW showed an actual vapor condensation rate of only 0.21 kg $m^{-2}h^{-1}$ while for rGO-TA-TW, the vapor condensation rate significantly increased to 0.67 kg $m^{-2}h^{-1}$ (Fig. 3a). After ceasing solar illumination, 16 h of vapor condensation in dark condition showed that vapor condensation rate in dark was only 0.06 kg $m^{-2}h^{-1}$ (Fig. S7). The concentrations of the four main cations (Na^+, K^+, Ca^{2+}, and Mg^{2+}) in the collected condensed water were drastically decreased compared to those in seawater and were far below the World Health Organization (WHO) standard threshold for drinkable desalinated water (Fig. 3b). This indicated that the collected clean water could be used as daily drinking water as well as irrigation for plant growth. Broccoli, a common green vegetable, grew normally following daily irrigation using the collected condensed water (Fig. 3c). Once watering ceased, the plants became dehydrated and did not survive properly (Fig. S8-9). In contrast, seeds directly watered with seawater failed to germinate (Fig. 3d) due to cell dehydration in a salt solution [13].

To realize *in-situ* utilization of the as-generated clean water from ISE for plant irrigation, a DVSSF system composed of a solar-thermal seawater desalination chamber (bottom layer), and a plant growth chamber (top layer) was designed (Fig. 3e and Fig. S10). Several water belts were placed on the back inner wall of the DVSSF to effectively transfer condensed clean water from the solar evaporation chamber to the plant growth chamber by capillary force, realizing automatic water supply. Under sunlight irradiation, plants on the upper layer consume water by photosynthesis and transpiration, and at the same time, the photothermal evaporators in the bottom chamber absorb sunlight for seawater evaporation and clean water production. The whole process is spontaneous without any human intervention. A device without photothermal evaporators was also fabricated for comparison. The results confirmed that the introduction of the photothermal evaporators significantly improved seawater evaporation. In the prototype device condensed water was clearly observed on the inner wall within 30 min, while for the control experiment without evaporators, no obvious condensed water was observed (Fig. S11). A long-term indoor test was also conducted to verify the feasibility of the DVSSF. The change in soil water content during the test is presented in Fig. 3f. During the first 9

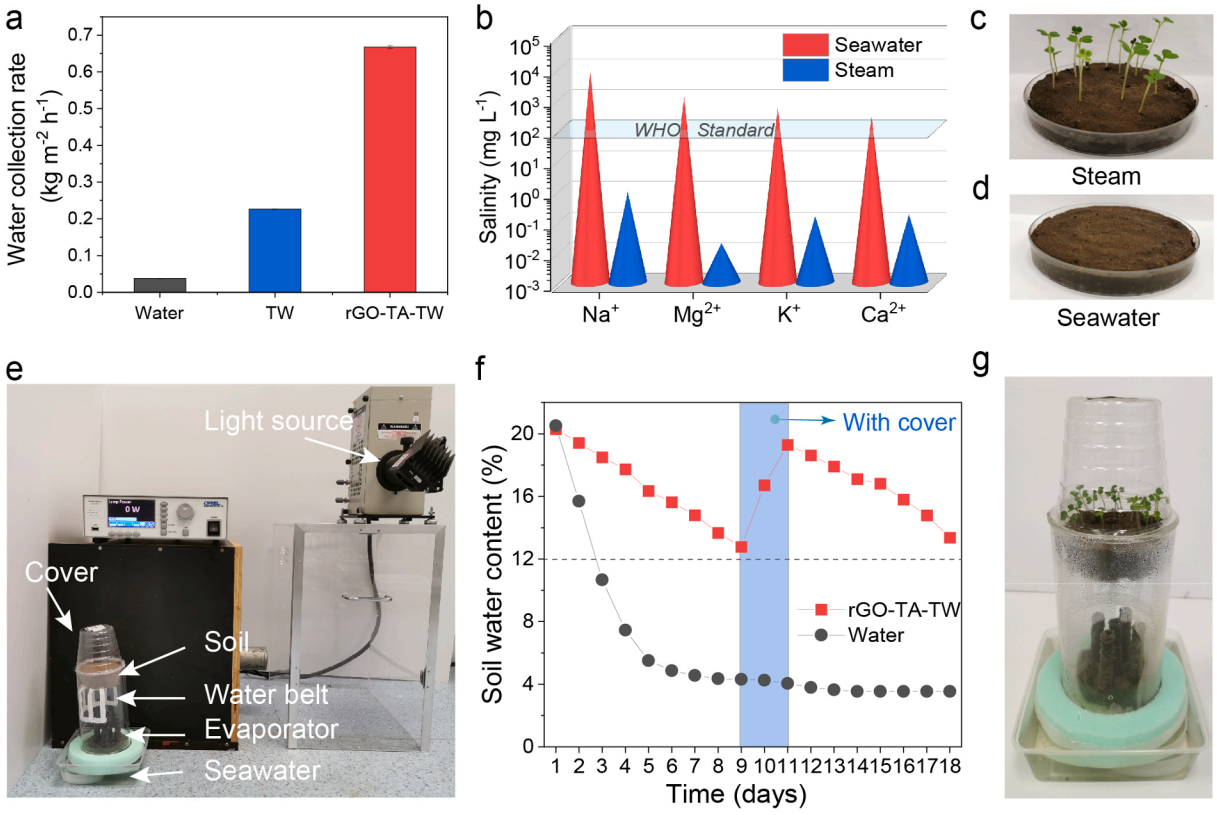

Fig. 3. Indoor tests. (**a**) Clean water collection rates from solar evaporation of seawater. (**b**) Salinities of seawater and the collected condensed water. (**c-d**) Seed germination performance with irrigation using condensed water from ISE and seawater. (**e**) Photograph of the indoor test setup with the DVSSF and seawater. (**f**) The change in soil water content during long-term indoor test with illumination (8 h per day) or under dark conditions. (**g**) Plant growth status on day 11.

days, without a cover the soil water content decreased steadily under light illumination. It is worth noting that under solar illumination, the soil water content with the ISE system beneath dropped more slowly compared to the system in dark conditions due to the quick water supply from the ISE chamber. After 9 days, the soil water content was still above 12% and remained suitable for plant growth. When a cover was added for the next 2 days, the soil water content quickly increased and returned to its initial level. The soil water content started to decrease again when the cover was removed on day 11. In comparison, long-term dark evaporation demonstrated that soil water content quickly dropped from 20% to 12% in 4 days (Fig. 3f and Fig. S12), where a low soil water content is not conducive to seed germination and growth [57]. Although the environmental conditions (i.e., indoor temperature and humidity) fluctuated during the long-term tests, they did not have a significant impact on the soil water content within the DVSSF (Fig. S13). Comparative experiment with initially dry soil showed that with the cover, the surface of the dry soil could be quickly moistened by the generated clean water within only 2 days of light illumination. While without the cover, there was no obvious change in the dry soil surface (Fig. S14). Plant germination was also evaluated during this long-term indoor experiment. It was clear that with light illumination the plants were able to grow normally due to the water supply from beneath ISE and suitable soil water content (Fig. 3g and Fig. S15), clearly proving the feasibility of the vertical solar sea farm design. Too much or too little water will affect the growth of plants. The soil water content could be maintained in a certain range suitable for plant growth by adjusting the open rate of the cover. To prevent clean water wastage, an additional freshwater collection container can be incorporated within the evaporation chamber to collect excessive clean water generated. The humidity in the top chamber also can be regulated by adjusting the cover. These measures can maintain a balance between water supply and consumption for plant growth.

3.3. Outdoor long-term germination performance in DVSSF

Four different DVSSF systems were prepared for long-term outdoor tests, including DVSSF I) without either water belts or photothermal evaporators; DVSSF II) with water belts but without photothermal evaporators; DVSSF III) without water belts but with photothermal evaporators; and DVSSF IV) with both water belts and photothermal evaporators (Fig. 4a). Outdoor tests were conducted at Mawson Lakes Campus, UniSA, South Australia over two weeks using seawater. The humidity and temperature inside the planting chamber of each DVSSF and the corresponding external environment parameters were recorded (Fig. S16). The temperature inside the DVSSF IV was typically below 40 ℃ (Fig. S16a). It is worth mentioning that conventional floating farms are generally enclosed systems, and where continuous solar energy input during solar seawater evaporation and vapor condensation often leads to overheating of the system [13]. In comparison, our DVSSF enabled continuous seawater evaporation and vapor condensation, while simultaneously maintaining suitable environmental conditions for plant growth due to the spatial separation of the lower solar evaporation

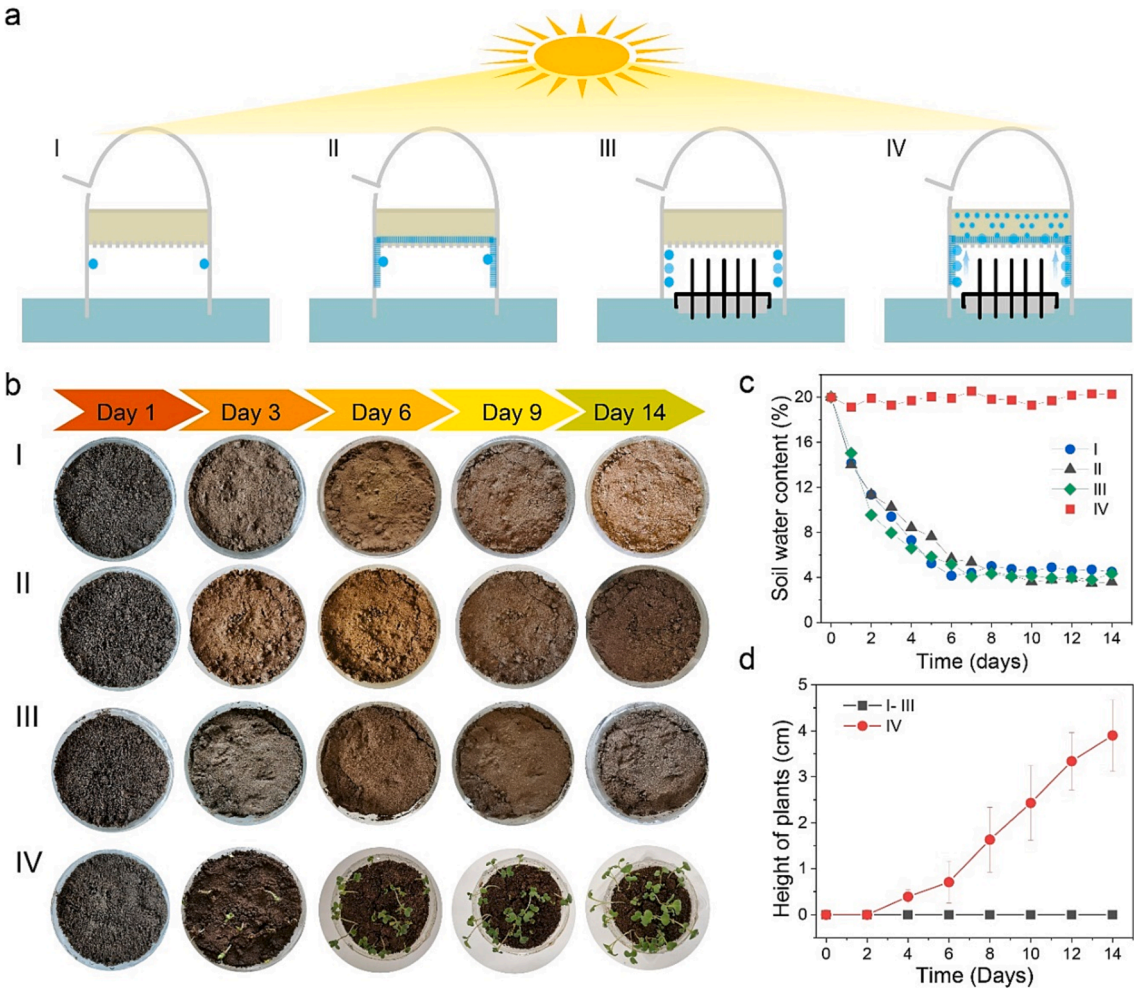

Fig. 4. Outdoor tests. (**a**) Schematic illustration of difference designs of DVSSFs. (**b**) Photographs of the soil surface during long-term outdoor tests. (**c**) Temporal variation in soil water content in the four DVSSFs. (**d**) Temporal variation in plant heights during long-term outdoor tests.

chamber and the upper plant cultivation chamber. During outdoor tests, the temperature reached a peak value at around 1 pm every day, and the internal humidity was constantly stabilized at ~ 80% in 14 days, despite a lower external environmental humidity (Fig. S16b), indicating adequate soil water content for plant growth. For the other three DVSSFs, such as DVSFF I, while the temperature did not significantly change, after commencing the experiment, the humidity in the cultivation chamber continually decreased, becoming similar (<40%) to the external humidity after three days (Fig. S16c-d). Comparison between measured ambient temperature and humidity with those sources from local monitoring station were highly correlated, suggesting that the monitoring station data can be directly used as an accurate reference (Fig. S17). Observation of the soil surface during tests (Fig. 4b) showed that in DVSSF I-III the soil surfaces dried out within 3 days, and were thoroughly dried and cracked after 14 days, resulting in no seed germination. In contrast, in DVSSF IV the soil surface was always wet, leading to excellent seed germination (Fig. S18). The measured soil moisture content in DVSSF I-III decreased continuously and remained at around 5% after 10 days. In comparison, for DVSSF IV, the soil water content remained relatively steady near 20% for the entire14 days

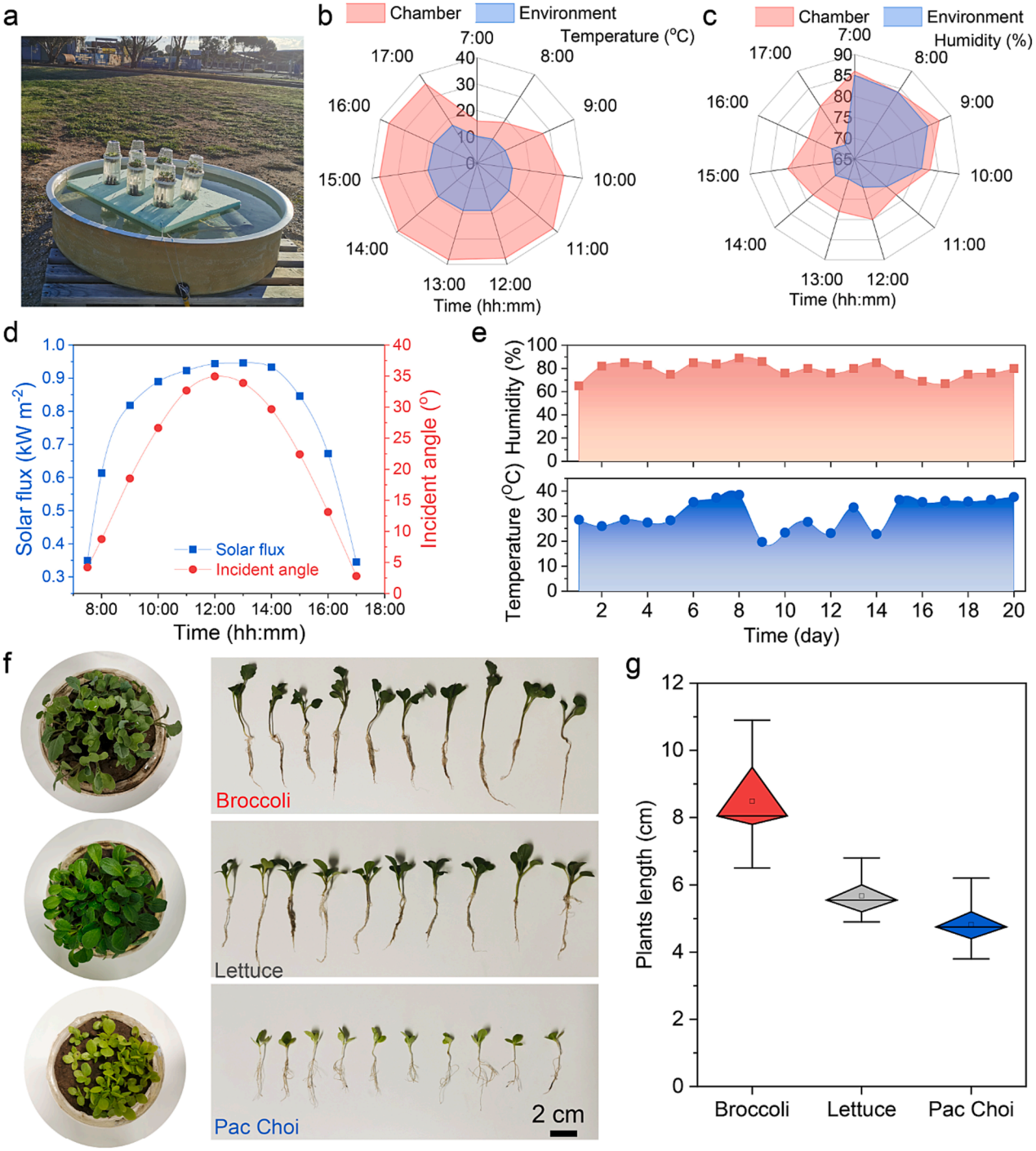

Fig. 5. Scale-up outdoor tests. (**a**) Photograph of experimental setup. (**b, c**) Daytime comparison of outdoor environmental conditions and conditions inside the DVSSF chamber. (**d**) Temporal variation in daytime solar flux and incident angle. (**e**) Twenty-day variation in chamber humidity and temperature at 1 pm. (**f**) Photographs of cultivated seedings. (**g**) Plants length 20 days after gemination.

(Fig. 4c). Broccoli seeds in DVSSF IV started to germinate only 3 days after the commencement of tests, and continued to grow well, reaching a height of about 4 cm after 2 weeks, confirming successfully sustained plant cultivation (Fig. 4d). Thus, a DVSSF system possessing both photothermal evaporators and water belts (i.e., device IV) is suitable for practical applications.

In practical applications, weather conditions such as sunlight intensity, incident angle and environmental temperature also affected the water production rate [34]. During the outdoor tests, solar exposure data collected from the local bureau of meteorology (Fig. S19) was used to calculate the appropriate angle of incidence for the DVSSF design (Fig. S20). The 3D evaporators would be completely exposed to sunlight when the angle of incidence was $< 45.0^{\circ}$. During the long-term outdoor tests, there were only about 2 h in a day when the incident angle was $> 45^{\circ}$, confirming that the evaporators in the DVSSF could effectively capture natural incident sunlight to ensure ISE processes. It should be mentioned that since the angle of incident sunlight varies with geographic region, the final DVSSF configuration should be adjusted to suit such local environmental features and to ensure efficient sunlight harvest.

3.4. Scale-up vertical farming system

Following the initial success of the prototype system described above, relatively large-scale outdoor experiments using three different plant types were also verified at UniSA (Mawson Lake Campus) from 4th to 23rd May 2022. Specifically, a large pool (1 m^2) with artificial seawater (Table S2) and six DVSSFs with three different seeds (two each for broccoli, lettuce, and Pak Choi) were prepared (Fig. 5a). Environmental conditions (i.e., temperature and humidity) and the associated plant cultivation chamber conditions were recorded from 7 am to 5 pm on May 21, 2022. The temperature inside the device was always higher than the environmental temperature (Fig. 5b), where appropriately elevated temperature benefited plants growth [58]. At 7 am the initial chamber humidity (85%) was similar to the environmental humidity (84%). Thereafter, while the environmental humidity exhibited a significant daily fluctuation (significantly decreasing throughout the day), the humidity inside the chamber remained constant at ~ 80% (Fig. 5c). Measurements of temporal variation in daytime solar flux and incident angle (Fig. 5d) demonstrated that a higher incident angle resulted in a higher solar flux between 11:00 am and 14:00 pm, where both light intensity and angle of incidence reached maxima of 0.95 sun and 35°, respectively at about 1:00 pm.

Correspondingly, when the solar flux reached its maxima, despite the low external environmental humidity, the internal humidity could be maintained at ~ 75% during the 20 days tests (Fig. 5e and Fig. S21). In addition, the internal temperature in the chamber was maintained lower than 40°, which ensured normal plant growth. Plant assays showed that during the tests, all broccoli, lettuce, and Pak Choi grew well exhibiting different plant dependent lengths (Fig. 5f-g, Fig. S22-23), and all three plants had germination rates > 80% (Fig. S24). Therefore, this DVSSF could provide simultaneous offshore solar-driven production of clean water and crops, thus providing a new pathway for sustainable marine farming.

While this work has successfully demonstrated the applicability of the DVSSF, there is still some room for improvement. For example, in this DVSSF clean water production by ISE was actually surplus for soil and plant irradiation. Therefore, it is desirable that any excess clean water generated *in situ* could be collected and stored for other applications. The feasibility and stability of this design were further validated through long-term outdoor experiments. However, for practical large-scale applications, shielding may occur. To solve this potential issue, monitoring and managing plant growth are required to prevent excessive occlusion of the evaporator. Furthermore, selecting plant species with suitable growth characteristics can minimize light-blocking effects. Additionally, adjusting the dimension of solar sea farm and the interspace between the devices, as well as incorporating light-reflection surfaces are also effective pathways to ensure sufficient sunlight access. The photothermal material could also be replaced with cheaper alternatives such as biochar and carbon black. Especially considering the themes of energy saving and emission reduction, the utilization of these low-cost and environmentally friendly materials should have great potential for future large-scale practical applications. In addition, although this design does not require ongoing maintenance and is well suited to many areas with mild weather conditions, quick and drastic changes in environmental conditions may affect the conditions in the DVSSF and consequently plant growth. Therefore, intelligent control systems can be introduced to further improve the stability (i.e., temperature and humidity) of the systems [12,13].

4. Conclusions

The integration of interfacial solar seawater evaporation and self-irrigation processes has successfully demonstrated a self-sustained DVSSF system that can float on sea and/or salty water surfaces to produce clean water for crop growth, with the capacity to alleviate the severity of global water shortages and food insecurity. The system which is powered only by solar light, uses vertical multi-level functional partitioning to directly utilize seawater for clean water production, irrigation and agricultural production, greatly increasing space utilization efficiency. In the DVSSF, the lower solar evaporation chamber can produce sufficient clean water and automatically real-time transfer the clean water to the upper growth chamber for soil and crop irrigation, enabling > 80% germination rate and good plant growth thereafter. This vertical farming design with minimal geological constrain can provide a promising way for agricultural irrigation to occur on many water bodies including seawater, rivers and salt lakes. This approach has great potential to significantly improve the global water-energy-food nexus, providing new solutions to the existing freshwater, land and food crises.

Declaration of Competing Interest

The authors declare that they have no known competing financial interests or personal relationships that could have appeared to influence the work reported in this paper.

Data availability

Data will be made available on request.

Acknowledgements

H.X. and G.O. acknowledge the financial support from the Australian Research Council (FT190100485, DP220100583). P.W. J.Z. and Y.W. acknowledge financial support from the China Scholarship Council for their primary scholarships and from the Future Industries Institute for top up scholarships. All authors acknowledge the use of the SA node of the NCRIS-enabled Australian National Fabrication Facility (ANFF).

Appendix A. Supplementary data

Supplementary data to this article can be found online at https://doi.org/10.1016/j.cej.2023.145452.

References

[1] J. Yang, X. Zhang, H. Qu, Z.G. Yu, Y. Zhang, T.J. Eey, Y.W. Zhang, S.C. Tan, A moisture-hungry copper complex harvesting air moisture for potable water and autonomous urban agriculture, Adv. Mater. 32 (2020) e2002936.

[2] S.H. van Delden, M. SharathKumar, M. Butturini, L.J.A. Graamans, E. Heuvelink, M. Kacira, E. Kaiser, R.S. Klamer, L. Klerkx, G. Kootstra, A. Loeber, R.E. Schouten, C. Stanghellini, W. van Ieperen, J.C. Verdonk, S. Vialet-Chabrand, E.J. Woltering, R. van de Zedde, Y. Zhang, L.F.M. Marcelis, Current status and future challenges in

implementing and upscaling vertical farming systems, Nat. Food 2 (2021) 944–956, https://doi.org/10.1038/s43016-021-00402-w.
[3] R.Y. Li, M.C. Wu, S. Aleid, C.L. Zhang, W.B. Wang, P. Wang, An integrated solar-driven system produces electricity with fresh water and crops in arid regions, Cell Rep. Phys. Sci. 3 (2022), 100781, https://doi.org/10.1016/j.xcrp.2022.100781.
[4] R.R. Hernandez, A. Armstrong, J. Burney, G. Ryan, K. Moore-O'Leary, I. Diédhiou, S.M. Grodsky, L. Saul-Gershenz, R. Davis, J. Macknick, D. Mulvaney, G.A. Heath, S. B. Easter, M.K. Hoffacker, M.F. Allen, D.M. Kammen, Techno–ecological synergies of solar energy for global sustainability, Nat. Sustain. 2 (7) (2019) 560–568.
[5] Z. Zhao, D. Wang, P. Gan, Y. Li, M. Tong, J. Liang, Solar-driven atmospheric water harvesting with a super-hygroscopic composite modified activated carbon fiber for tropical island ecological farm, Environ. Funct. Mater. 1 (2022) 275–283, https://doi.org/10.1016/j.efmat.2022.10.002.
[6] M. Zou, Y. Zhang, Z. Cai, C. Li, Z. Sun, C. Yu, Z. Dong, L. Wu, Y. Song, 3D printing a biomimetic bridge-arch solar evaporator for eliminating salt accumulation with desalination and agricultural applications, Adv. Mater. 33 (2021) e2102443.
[7] A. LaPotin, Y. Zhong, L. Zhang, L. Zhao, A. Leroy, H. Kim, S.R. Rao, E.N. Wang, Dual-stage atmospheric water harvesting device for scalable solar-driven water production, Joule 5 (2021) 166–182, https://doi.org/10.1016/j.joule.2020.09.008.
[8] X.Y. Zhou, P.P. Zhang, F. Zhao, G.H. Yu, Super moisture absorbent gels for sustainable agriculture via atmospheric water irrigation, ACS Mater. Lett. 2 (2020) 1419–1422, https://doi.org/10.1021/acsmaterialslett.0c00439.
[9] H. Qi, T. Wei, W. Zhao, B. Zhu, G. Liu, P. Wang, Z. Lin, X. Wang, X. Li, X. Zhang, J. Zhu, An interfacial solar-driven atmospheric water generator based on a liquid sorbent with simultaneous adsorption-desorption, Adv. Mater. (2019) e1903378.
[10] Z.W. Lei, S.F. Zhu, X.T. Sun, S.N. Yu, X.Q. Liu, K. Liang, X.J. Zhang, L.J. Qu, L. L. Wang, X.S. Zhang, A Multiscale porous 3D-fabric evaporator with vertically aligned yarns enables ultra-efficient and continuous water desalination, Adv. Funct. Mater. 32 (2022) 2205790, https://doi.org/10.1002/adfm.202205790.
[11] J.Y. Wang, C.H. Deng, G.D. Zhong, W.J. Ying, C.F. Li, S.G. Wang, Y.F. Liu, R. Z. Wang, H. Zhang, High-yield and scalable water harvesting of honeycomb hygroscopic polymer driven by natural sunlight, Cell Rep. Phys. Sci. 3 (2022), https://doi.org/10.1016/j.xcrp.2022.100954.
[12] X. Zhang, J. Yang, H. Qu, Z.G. Yu, D.K. Nandakumar, Y. Zhang, S.C. Tan, Machine-learning-assisted autonomous humidity management system based on solar-regenerated super hygroscopic complex, Adv. Sci. 8 (2021) 2003939, https://doi.org/10.1002/advs.202003939.
[13] S. Guo, Y.X. Zhang, H. Qu, M. Li, S.L. Zhang, J.C. Yang, X.P. Zhang, S.C. Tan, Repurposing face mask waste to construct floating photothermal evaporator for autonomous solar ocean farming, Ecomat 4 (2022) e12179.
[14] R. Li, Y. Shi, M. Wu, S. Hong, P. Wang, Photovoltaic panel cooling by atmospheric water sorption–evaporation cycle, Nat. Sustain. 3 (2020) 636–643, https://doi.org/10.1038/s41893-020-0535-4.
[15] P.H. Raven, D.L. Wagner, Agricultural intensification and climate change are rapidly decreasing insect biodiversity, Proc. Natl. Acad. Sci. 118 (2021), https://doi.org/10.1073/pnas.2002548117 e2002548117.
[16] R.R. Gentry, E.O. Ruff, S.E. Lester, Temporal patterns of adoption of mariculture innovation globally, Nat. Sustain. 2 (2019) 949–956, https://doi.org/10.1038/s41893-019-0395-y.
[17] Q. Wang, Z. Zhu, G. Wu, X. Zhang, H. Zheng, Energy analysis and experimental verification of a solar freshwater self-produced ecological film floating on the sea, Appl. Energy 224 (2018) 510–526, https://doi.org/10.1016/j.apenergy.2018.05.010.
[18] C. Chen, Y. Kuang, L. Hu, Challenges and Opportunities for Solar Evaporation, Joule 3 (2019) 683–718, https://doi.org/10.1016/j.joule.2018.12.023.
[19] P. Tao, G. Ni, C. Song, W. Shang, J. Wu, J. Zhu, G. Chen, T. Deng, Solar-driven interfacial evaporation, Nat. Energy 3 (2018) 1031–1041, https://doi.org/10.1038/s41560-018-0260-7.
[20] M. Gao, L. Zhu, C.K. Peh, G.W. Ho, Solar absorber material and system designs for photothermal water vaporization towards clean water and energy production, Energ. Environ. Sci. 12 (2019) 841–864, https://doi.org/10.1039/c8ee01146j.
[21] Y.X. Zhang, S.C. Tan, Best practices for solar water production technologies, Nat. Sustain. 5 (2022) 554–556, https://doi.org/10.1038/s41893-022-00880-1.
[22] J. Ma, L. An, D. Liu, J. Yao, D. Qi, H. Xu, C. Song, F. Cui, X. Chen, J. Ma, W. Wang, A light-permeable solar evaporator with three-dimensional photocatalytic sites to boost volatile-organic-compound rejection for water purification, Environ. Sci. Tech. 56 (2022) 9797–9805, https://doi.org/10.1021/acs.est.2c01874.
[23] C.T.K. Finnerty, A.K. Menon, K.M. Conway, D. Lee, M. Nelson, J.J. Urban, D. Sedlak, B. Mi, Interfacial solar evaporation by a 3D graphene oxide stalk for highly concentrated brine treatment, Environ. Sci. Tech. 55 (2021) 15435–15445, https://doi.org/10.1021/acs.est.1c04010.
[24] M. Li, B. Liu, H. Guo, H. Wang, Q. Shi, M. Xu, M. Yang, X. Luo, L. Wang, Reclaimable MoS(2) sponge absorbent for drinking water purification driven by solar energy, Environ. Sci. Tech. 56 (2022) 11718–11728, https://doi.org/10.1021/acs.est.2c03033.
[25] Y. Dong, Y. Tan, K. Wang, Y. Cai, J. Li, C. Sonne, C. Li, Reviewing wood-based solar-driven interfacial evaporators for desalination, Water Res. 223 (2022), 119011, https://doi.org/10.1016/j.watres.2022.119011.
[26] X. Li, W. Xie, J. Zhu, Interfacial solar steam/vapor generation for heating and cooling, Adv Sci (Weinh) 9 (2022) e2104181.
[27] X. Liu, F. Chen, Y. Li, H. Jiang, D.D. Mishra, F. Yu, Z. Chen, C. Hu, Y. Chen, L. Qu, W. Zheng, 3D hydrogel evaporator with vertical radiant vessels breaking the trade-off between thermal localization and salt resistance for solar desalination of high-salinity, Adv. Mater. 34 (2022) e2203137.
[28] H. Mo, Y. Wang, A bionic solar-driven interfacial evaporation system with a photothermal-photocatalytic hydrogel for VOC removal during solar distillation, Water Res. 226 (2022), 119276, https://doi.org/10.1016/j.watres.2022.119276.
[29] Z.H. Zheng, H. Liu, D.Z. Wu, X.D. Wang, Polyimide/MXene hybrid aerogel-based phase-change composites for solar-driven seawater desalination, Chem. Eng. J. 440 (2022), 135862, https://doi.org/10.1016/j.cej.2022.135862.
[30] H.M. Zhang, X. Shen, E.Y. Kim, M.Y. Wang, J.H. Lee, H.M. Chen, G.C. Zhang, J. K. Kim, Integrated water and thermal managements in bioinspired hierarchical MXene aerogels for highly efficient solar-powered water evaporation, Adv. Funct. Mater. 32 (2022) 2111794, https://doi.org/10.1002/adfm.202111794.
[31] Z. Wang, J. Gao, J. Zhou, J. Gong, L. Shang, H. Ye, F. He, S. Peng, Z. Lin, Y. Li, F. Caruso, Engineering metal-phenolic networks for solar desalination with directional salt crystallization, Adv. Mater. 35 (2023) 2209015, https://doi.org/10.1002/adma.202209015.
[32] B. Shao, X. Wu, Y.D. Wang, T. Gao, Z.Q. Liu, G. Owens, H.L. Xu, A general method for selectively coating photothermal materials on 3D porous substrate surfaces towards cost-effective and highly efficient solar steam generation, J. Mater. Chem. A 8 (2020) 24703–24709, https://doi.org/10.1039/d0ta08539a.
[33] H. Yu, D. Wang, H. Jin, P. Wu, X. Wu, D. Chu, Y. Lu, X. Yang, H. Xu, 2D MoN1.2-rGO stacked heterostructures enabled water state modification for highly efficient interfacial solar evaporation, Adv. Funct. Mater. 33 (2023), https://doi.org/10.1002/adfm.202214828.
[34] P. Wu, X. Wu, Y. Wang, H. Xu, G. Owens, Towards sustainable saline agriculture: Interfacial solar evaporation for simultaneous seawater desalination and saline soil remediation, Water Res. 212 (2022), 118099, https://doi.org/10.1016/j.watres.2022.118099.
[35] X. Wu, Y. Wang, P. Wu, J. Zhao, Y. Lu, X. Yang, H. Xu, Dual-zone photothermal evaporator for antisalt accumulation and highly efficient solar steam generation, Adv. Funct. Mater. 31 (2021) 2102618, https://doi.org/10.1002/adfm.202102618.
[36] Y. Wang, X. Wu, P. Wu, J. Zhao, X. Yang, G. Owens, H. Xu, Enhancing solar steam generation using a highly thermally conductive evaporator support, Sci. Bull. 66 (2021) 2479–2488, https://doi.org/10.1016/j.scib.2021.09.018.
[37] L. Zhang, X. Li, Y. Zhong, A. Leroy, Z. Xu, L. Zhao, E.N. Wang, Highly efficient and salt rejecting solar evaporation via a wick-free confined water layer, Nat. Commun. 13 (2022) 849, https://doi.org/10.1038/s41467-022-28457-8.
[38] F. Wang, N. Xu, W. Zhao, L. Zhou, P. Zhu, X. Wang, B. Zhu, J. Zhu, A high-performing single-stage invert-structured solar water purifier through enhanced absorption and condensation, Joule 5 (2021) 1602–1612, https://doi.org/10.1016/j.joule.2021.04.009.
[39] P.C. Yao, H. Gong, Z.Y. Wu, H.Y. Fu, B. Li, B. Zhu, J.W. Ji, X.Y. Wang, N. Xu, C. J. Tang, H.G. Zhang, J. Zhu, Greener and higher conversion of esterification via interfacial photothermal catalysis, Nat. Sustain. 5 (2022) 348–356, https://doi.org/10.1038/s41893-021-00841-0.
[40] H. Ghasemi, G. Ni, A.M. Marconnet, J. Loomis, S. Yerci, N. Miljkovic, G. Chen, Solar steam generation by heat localization, Nat. Commun. 5 (2014) 4449, https://doi.org/10.1038/ncomms5449.
[41] F. Zhao, X. Zhou, Y. Shi, X. Qian, M. Alexander, X. Zhao, S. Mendez, R. Yang, L. Qu, G. Yu, Highly efficient solar vapour generation via hierarchically nanostructured gels, Nat. Nanotechnol. 13 (2018) 489–495, https://doi.org/10.1038/s41565-018-0097-z.
[42] Z. Yu, R. Gu, Y. Zhang, S. Guo, S. Cheng, S.C. Tan, High-flux flowing interfacial water evaporation under multiple heating sources enabled by a biohybrid hydrogel, Nano Energy 98 (2022), 107287, https://doi.org/10.1016/j.nanoen.2022.107287.
[43] N. Li, L. Luo, C. Guo, J.T. He, S.X. Wang, L.M. Yu, M. Wang, P. Murto, X.F. Xu, Shape-controlled fabrication of cost-effective, scalable and anti-biofouling hydrogel foams for solar-powered clean water production, Chem. Eng. J. 431 (2022), 134144, https://doi.org/10.1016/j.cej.2021.134144.
[44] W. Xie, P. Tang, Q. Wu, C. Chen, Z. Song, T. Li, Y. Bai, S. Lin, A. Tiraferri, B. Liu, Solar-driven desalination and resource recovery of shale gas wastewater by on-site interfacial evaporation, Chem. Eng. J. 428 (2022), 132624, https://doi.org/10.1016/j.cej.2021.132624.
[45] Y. Chen, J. Yang, L. Zhu, S. Wang, X. Jia, Y. Li, D. Shao, L. Feng, H. Song, Marangoni-driven biomimetic salt secretion evaporator, Desalination 548 (2023), https://doi.org/10.1016/j.desal.2022.116287.
[46] X. Mu, J. Zhou, P. Wang, H. Chen, T. Yang, S. Chen, L. Miao, T. Mori, A robust starch–polyacrylamide hydrogel with scavenging energy harvesting capacity for efficient solar thermoelectricity–freshwater cogeneration, Energ. Environ. Sci. 15 (2022) 3388–3399, https://doi.org/10.1039/d2ee01394k.
[47] T. Gao, Y. Wang, X. Wu, P. Wu, X. Yang, Q. Li, Z. Zhang, D. Zhang, G. Owens, H. Xu, More from less: improving solar steam generation by selectively removing a portion of evaporation surface, Sci. Bull. 67 (2022) 1572–1580, https://doi.org/10.1016/j.scib.2022.07.004.
[48] C. Lei, W. Guan, Y. Guo, W. Shi, Y. Wang, K.P. Johnston, G. Yu, Polyzwitterionic hydrogels for highly efficient high salinity solar desalination, Angew. Chem. Int. Ed. Engl. 61 (2022), https://doi.org/10.1002/anie.202208487 e202208487.
[49] J.Y. Zhao, X. Wu, H.M. Yu, Y.D. Wang, P. Wu, X.F. Yang, D.W. Chu, G. Owens, H. L. Xu, Regenerable aerogel-based thermogalvanic cells for efficient low-grade heat harvesting from solar radiation and interfacial solar evaporation systems, Ecomat 5 (2023) e12302.
[50] P. Wu, X. Wu, Y.D. Wang, H.L. Xu, G. Owens, A biomimetic interfacial solar evaporator for heavy metal soil remediation, Chem. Eng. J. 435 (2022), 134793, https://doi.org/10.1016/j.cej.2022.134793.

[51] Z.X. Wang, X.C. Wu, F. He, S.Q. Peng, Y.X. Li, Confinement capillarity of thin coating for boosting solar-driven water evaporation, Adv. Funct. Mater. 31 (2021) 2011114, https://doi.org/10.1002/adfm.202011114.
[52] Z. Wang, X. Wu, J. Dong, X. Yang, F. He, S. Peng, Y. Li, Porifera-inspired cost-effective and scalable "porous hydrogel sponge" for durable and highly efficient solar-driven desalination, Chem. Eng. J. 427 (2022), 130905, https://doi.org/10.1016/j.cej.2021.130905.
[53] L. Wang, Q. He, H.H. Yu, R.H. Jin, H.F. Zheng, A floating planting system based on concentrated solar multi-stage rising film distillation process, Energ. Conver. Manage. 254 (2022), https://doi.org/10.1016/j.enconman.2022.115227.
[54] Y. Wang, X. Sun, S. Tao, Rational 3D Coiled Morphology for Efficient Solar-Driven Desalination, Environ. Sci. Tech. 54 (2020) 16240–16248, https://doi.org/10.1021/acs.est.0c05449.
[55] P. Wu, X. Wu, H. Xu, G. Owens, Interfacial solar evaporation driven lead removal from a contaminated soil, EcoMat 3 (2021) e12140.
[56] Z. Wang, M. Han, F. He, S. Peng, S.B. Darling, Y. Li, Versatile coating with multifunctional performance for solar steam generation, Nano Energy 74 (2020), 104886, https://doi.org/10.1016/j.nanoen.2020.104886.
[57] B. Wen, Effects of high temperature and water stress on seed germination of the invasive species Mexican sunflower, PLoS One 10 (2015) e0141567.
[58] E. Fernández-Pascual, A. Carta, A. Mondoni, L.A. Cavieres, S. Rosbakh, S. Venn, A. Satyanti, L. Guja, V.F. Briceño, F. Vandelook, E. Mattana, A. Saatkamp, H. Bu, K. Sommerville, P. Poschlod, K. Liu, A. Nicotra, B. Jiménez-Alfaro, The seed germination spectrum of alpine plants: a global meta-analysis, New Phytol. 229 (2021) 3573–3586, https://doi.org/10.1111/nph.17086.